

Radioisotope Geochemistry

An Introduction

- Variety of naturally occurring and anthropogenic radioisotopes can be used to provide information on a wide variety of processes
- Can be used as tracers in same manner as stable isotopes but have the advantage of **time** as a parameter
- Their use requires certain assumptions be made – must be assessed on a case by case basis

Examples of Processes

- Water Column Vertical and Horizontal Transport by
 - Mixing
 - Particle Scavenging and Sedimentation
 - Lateral advection
- Sediment Accumulation & Dating
 - Accumulation Rates
 - Mixing
 - Resuspension

Modes of Decay

- Alpha(α) – emission of two neutrons and two protons together as helium ion from nucleus
- Beta (β) – emission of electron *from nucleus* resulting in increase in atomic number of 1 in original nucleus
- Gamma (γ) – emission of photons from excited nuclei

Basic Equations of Decay

$$N = N_0 e^{-\lambda t}$$

Where N_0 = number of atoms at $t = 0$

N = number of atoms at time = t

λ = first order rate (decay) constant

λN = Activity (Bq (= dps) or dpm unit used)

Decay Equations (cont.)

$$\ln N = \ln N_0 - \lambda t$$

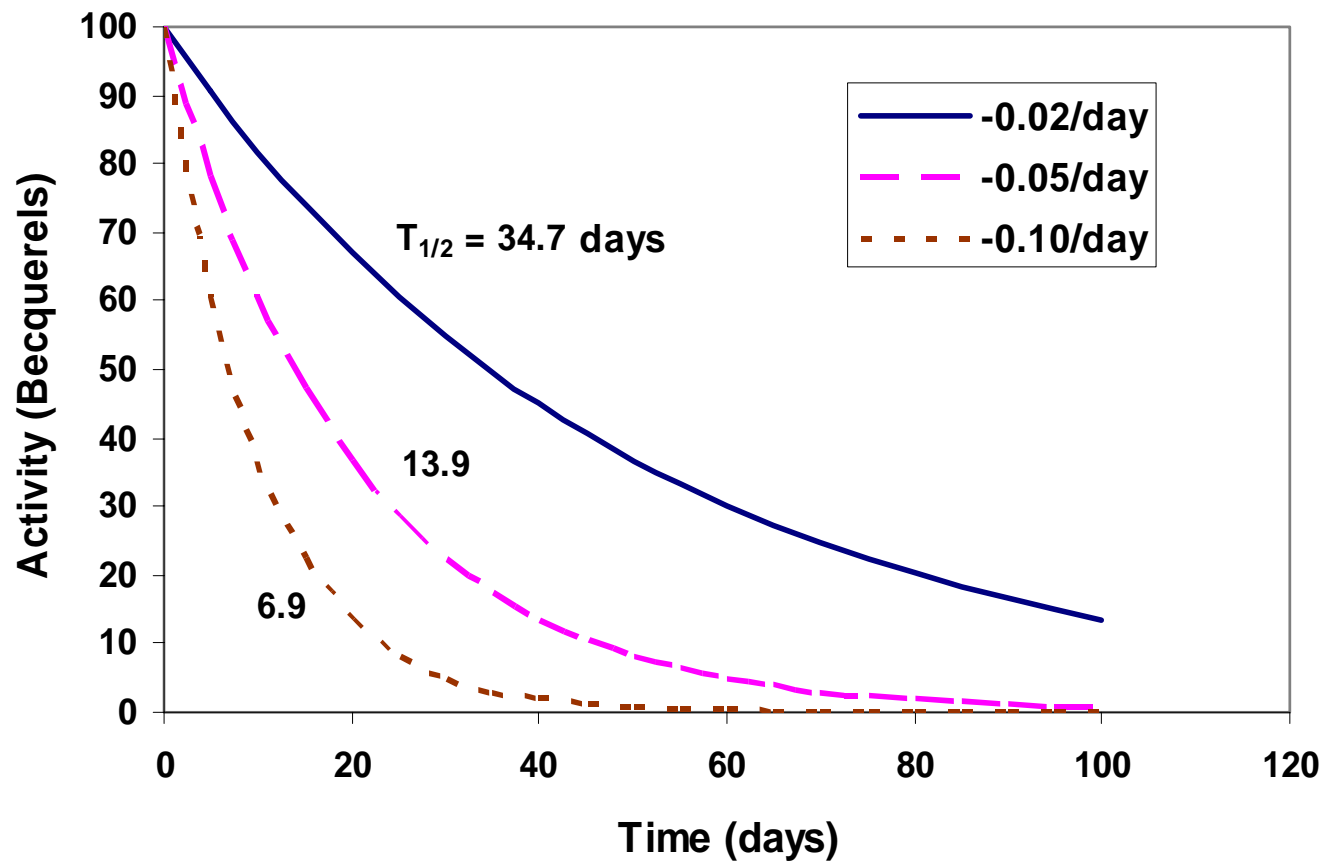
$$\text{When } N = \frac{1}{2} N_0$$

$$t = t_{1/2}$$

$$\text{i.e. } \ln 0.5 = -\lambda t_{1/2}$$

$$t_{1/2} = 0.693/\lambda$$

Decay



Classes of Radioisotopes

1. Primordial

- Parents produced by super-novae, long-lived
- not produced on earth
- e.g. U-series

2. Cosmogenic

- Produced by interaction of cosmic rays with atoms in the atmosphere or land surface
- Short to long-lived
- e.g. ^{14}C

3. Artificial

1. Man-made
2. Purposefully or incidentally (nuclear bombs)
3. e.g. ^{239}Pu

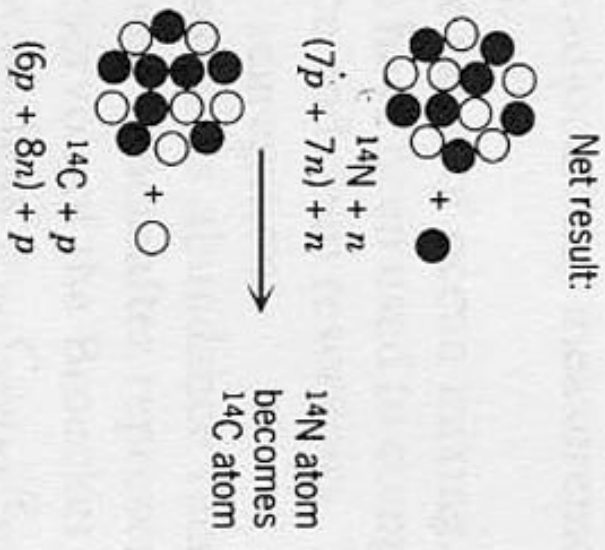
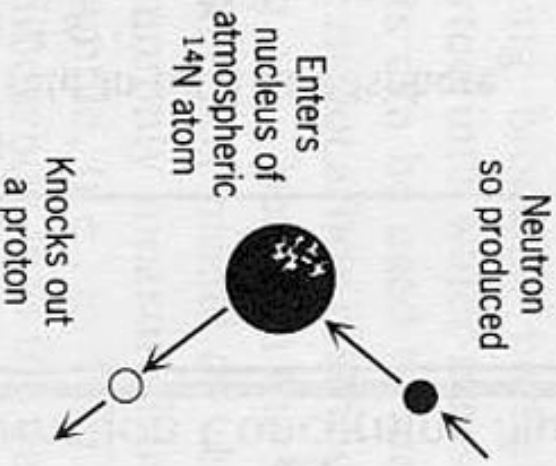
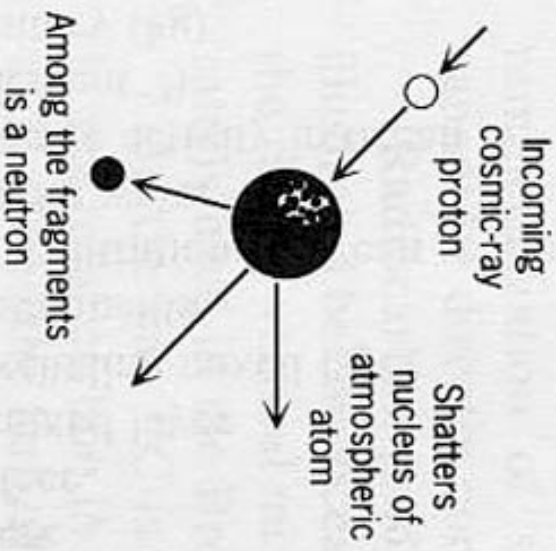
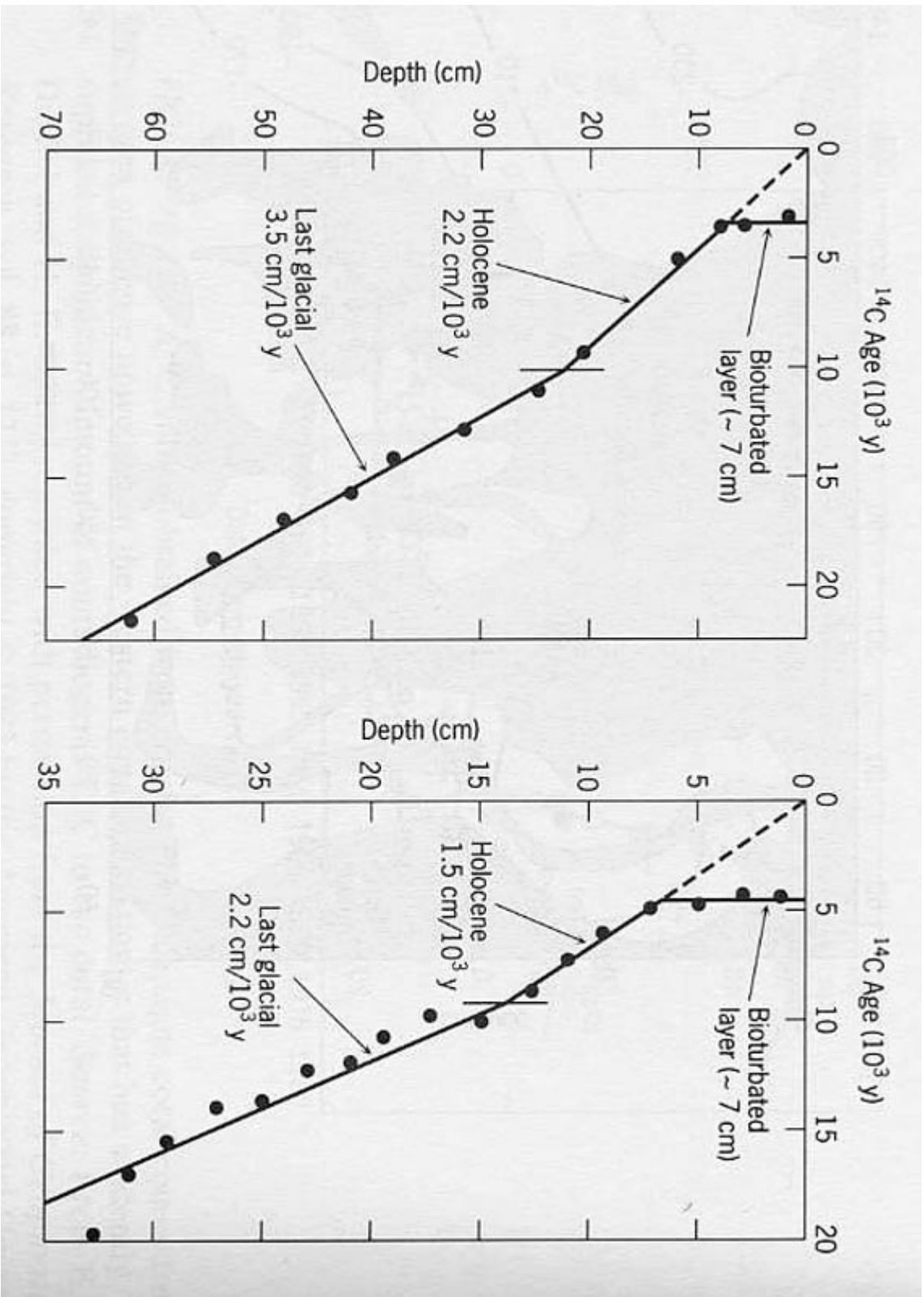


TABLE 28.6
Basic Information Concerning Nuclides Produced by Cosmic Rays

	Nuclide					
	3H	7Be	^{10}Be	^{14}C	^{26}Al	^{32}Si
Half-life (y)	12.3	0.145	2.5×10^6	5680	7.4×10^5	500
Production rate in total atmosphere (atom $cm^{-2} s^{-1}$)	0.25	0.081	0.045	2.5	1.4×10^{-4}	1.6×10^{-4}
Fraction of total earth inventory in						
Atmosphere	0.072	0.71	3.9×10^{-7}	0.019	1.4×10^{-6}	2.0×10^{-3}
Land surface	0.27	0.08	0.29	0.04	0.29	0.29
Ocean—mixed layer	0.35	0.2	5.7×10^{-6}	0.022	1.4×10^{-5}	0.0035
Ocean—excluding mixed layer	0.3	0.002	10^{-4}	0.92	7×10^{-5}	0.68
Oceanic sediments	0	0	0.71	0.004	0.71	0.028
Average concentration in ocean (10^{-3} dpm kg water $^{-1}$)	36	—	10^{-3}	260	1.2×10^{-5}	2.4×10^{-2}
Average specific activity in ocean (dpm g element $^{-1}$)	3.3×10^{-4}	—	1600	10	0.0012	0.008
Global inventory (kg)	3.5	3.2×10^{-3}	4.3×10^5	7.5×10^4	1.1×10^3	1.4
Global inventory (MCI)	35	1.1	6.4	340	0.020	0.023

Source: From *Chemical Oceanography*, vol. 3, J. D. Burton (eds; J. P. Riley and G. Skirrow), copyright © 1975 by Academic Press, Orlando, FL, p. 140. Reprinted by permission. Data from *The Handbook of Physics*, 2E, E. U. Condon and H. Odishaw, copyright © 1967 by McGraw-Hill, Inc., New York, pp. 9.277, 9.285, 9.319. Reprinted by permission.



Hughen et al. Science 2004; Cariaco Basin sediment ^{14}C

1) Annual laminations in this anoxic basin allows for ‘tree-ring’ year counting for much of the record

2. Difference between calendar year and ^{14}C age due to:

- ^{14}C production rate in atmosphere
- Deep mixing rate

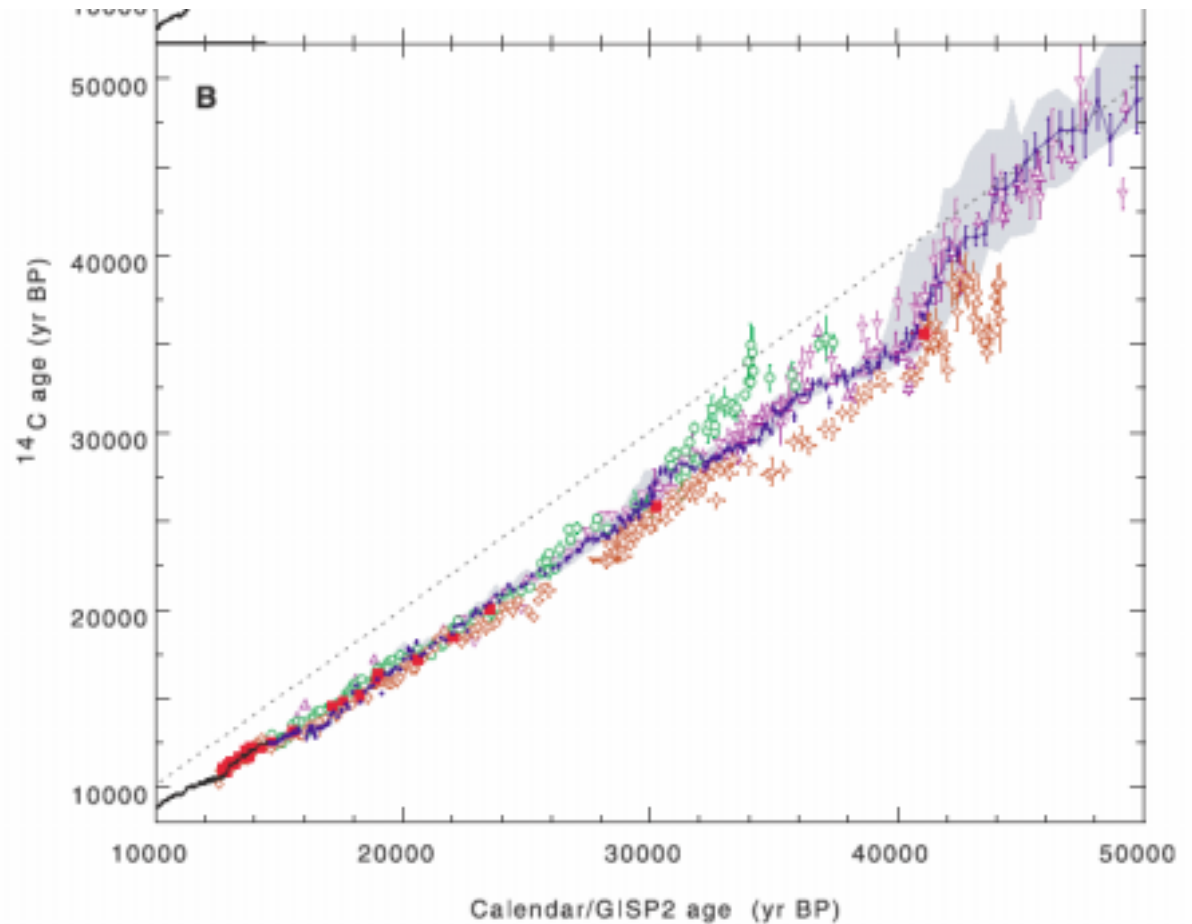


Fig. 2. Radiocarbon calibration data from various sources. (A) Calibration data from Cariaco leg 165, holes 1002D and 1002E (blue circles), plotted versus GISP2 calendar age (12) assigned by correlation of detailed paleoclimate records (17) (SOM Text and fig. S2). The thin black line is high-resolution calibration data from Intcal98 tree rings (2, 3) joined at ~ 12 cal. ka B.P. to the Cariaco PL07-58PC varve chronology (13). Red squares are paired ^{14}C -U/Th dates from corals (5). Replicate measurements, including overlap between 1002D and 1002E, have been averaged. Light gray shading represents the Cariaco calibration curve shifted within limits of calendar age uncertainty. Dashed line shows equal ^{14}C -calendar ages. Error bars are 1σ . (B) Cariaco site 1002 data set plotted versus other published ^{14}C calibration data. Symbols are the same as above, with additional data from Lake Suigetsu varves (6) (open circles), Bahama speleothem U/Th (7) (open diamonds), and North Atlantic cores PS2644 (9) (upside-down triangles) and SO82-5 (10) (triangles) correlated to GISP2. Error bars for all records are 1σ .

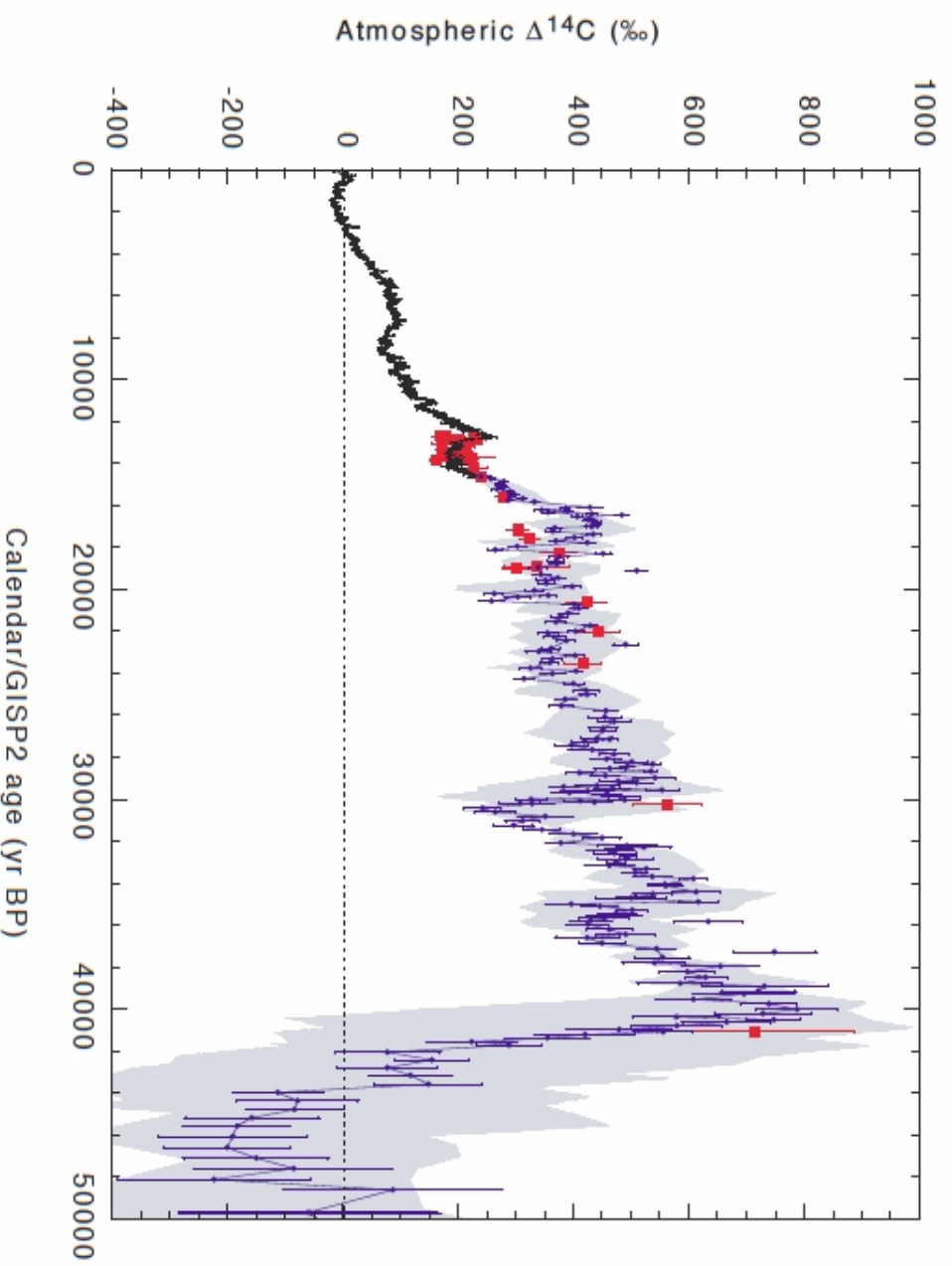
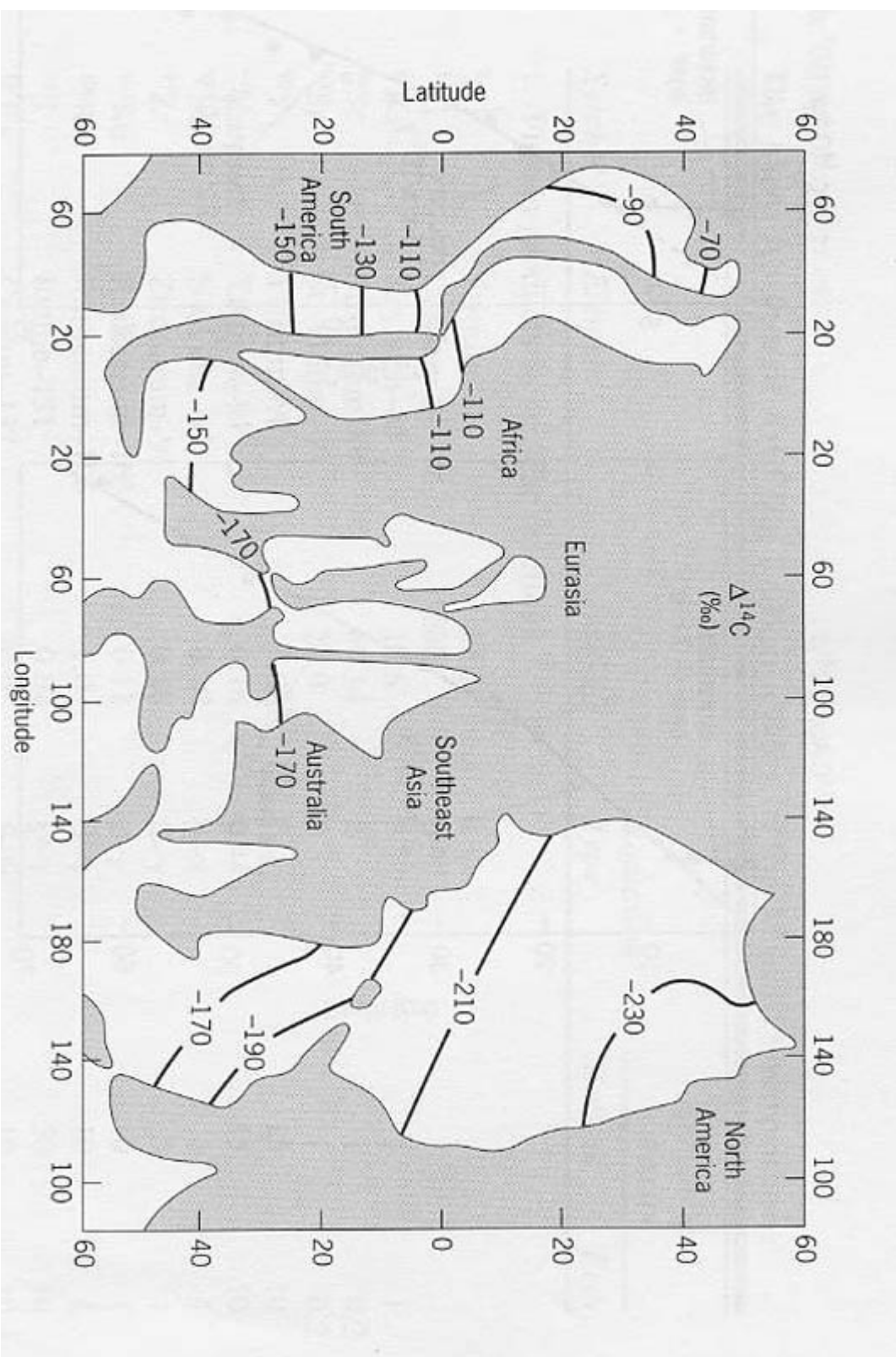
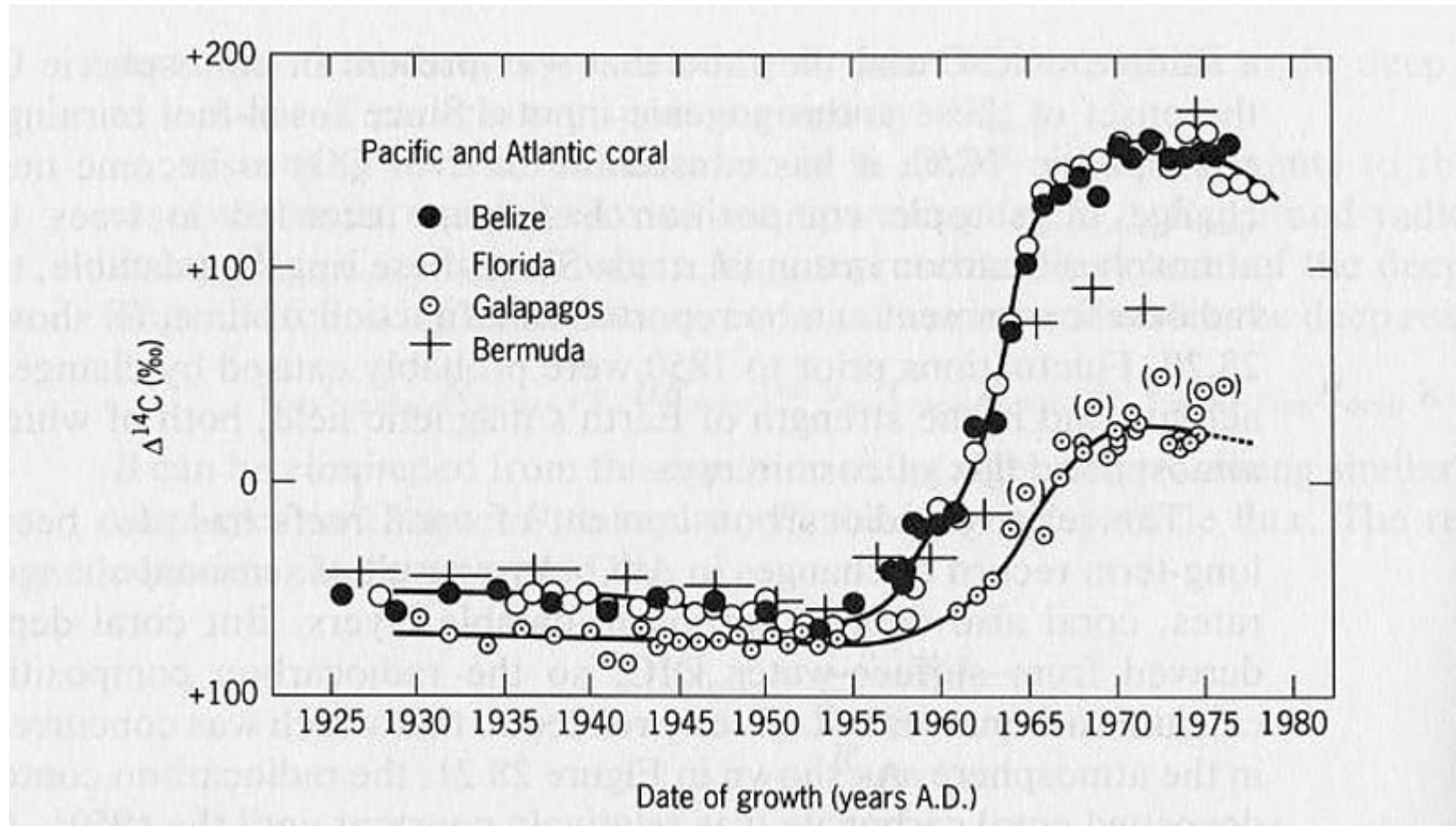


Fig. 3. Atmospheric $\Delta^{14}\text{C}$ for the past 50 cal. ka B.P. Symbols are the same as those in Fig. 2A. Cariaco error bars represent independent uncertainty in $\Delta^{14}\text{C}$ due to $1\text{-}\sigma$ ^{14}C age error. Light gray shading shows additional uncertainty in Cariaco $\Delta^{14}\text{C}$ due to calendar-age error that is not independent from sample to sample, but rather would shift sections of the curve together within the limits of the shading. Dotted line is modern preindustrial atmospheric $\Delta^{14}\text{C}$, defined as 0‰. Upper and lower limits were determined by adding and subtracting $1\text{-}\sigma$ errors to the calendar age and recalculating $\Delta^{14}\text{C}$ with the use of the new calendar ages.



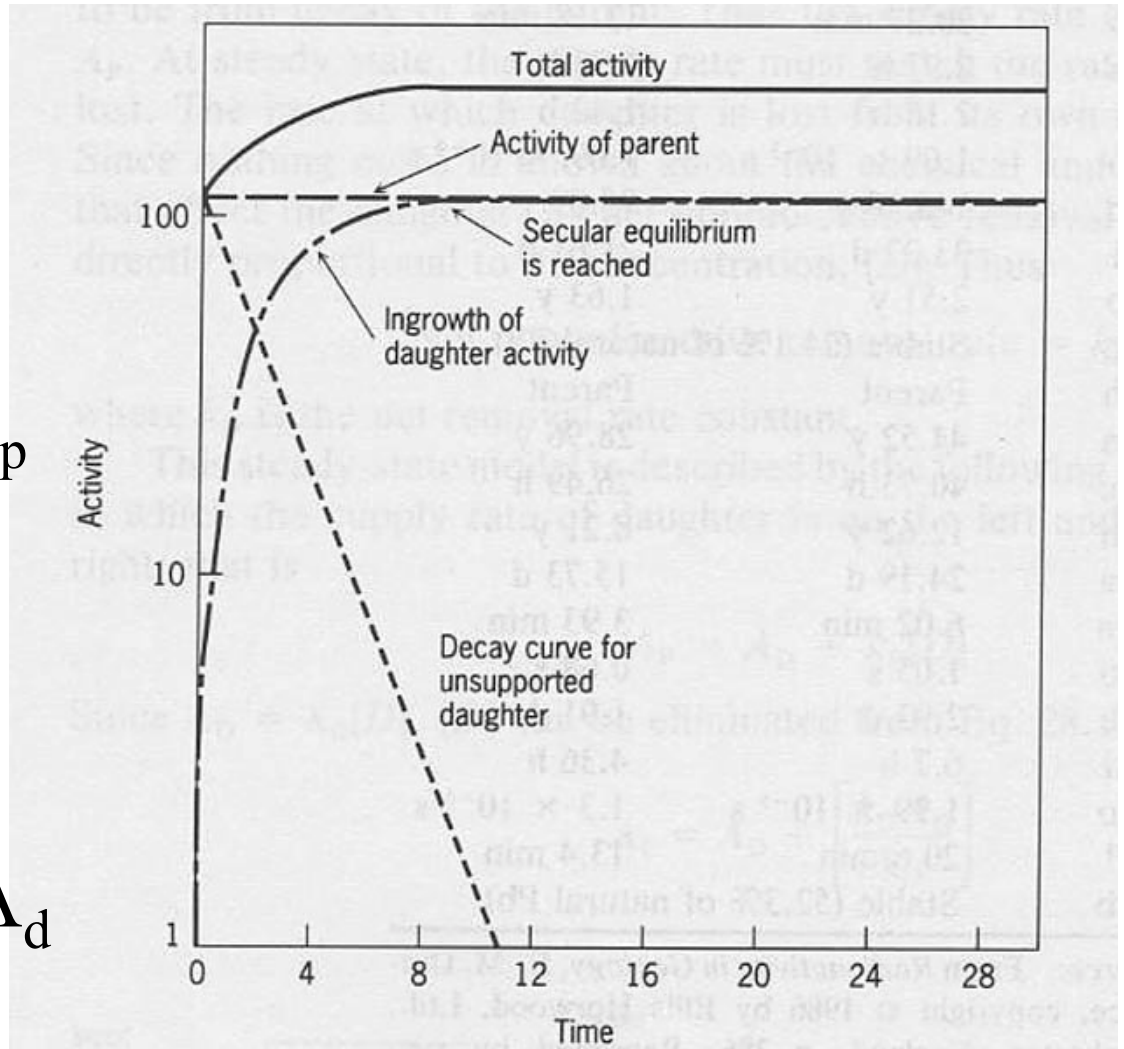
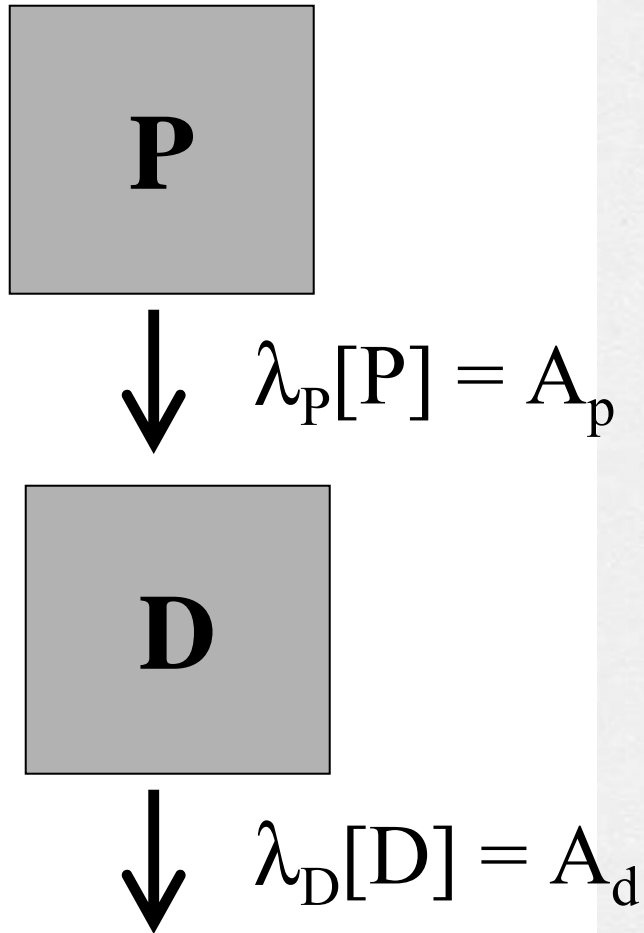
^{14}C also an 'artificial' radioisotope as a result of nuclear bomb testing



U-Th Decay Series

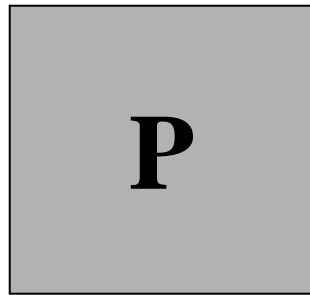
Element	U-238 series						Th-232 series				U-235 series				
Neptunium															
Uranium	U-238 4.47×10^9 y		U-234 2.48×10^5 y									U-235 7.04×10^8 y			
Protactinium		Pa-234 1.18 min											Pa-231 3.25×10^4 y		
Thorium	Th-234 24.1 d		Th-230 7.52×10^4 y				Th-232 1.40×10^{10} y		Th-228 1.91 y				Th-231 25.5 hrs		Th-227 18.7 d
Actinium								Ac-228 6.13 hrs					Ac-227 21.8 y		
Radium			Ra-226 1.62×10^3 y					Ra-228 5.75 y		Ra-224 3.66 d				Ra-223 11.4 d	
Francium															
Radon			Rn-222 3.82 d							Rn-220 55.6 s				Rn-219 3.96 s	
Astatine															
Polonium			Po-218 3.05 min		Po-214 1.64×10^{-4} s				Po-216 0.15 s	64%	Po-212 3.0×10^{-7} s			Po-215 1.78×10^{-3} s	
Bismuth				Bi-214 19.7 min		Bi-210 5.01 d				Bi-212 60.6 min					Bi-211 2.15 min
Lead			Pb-214 26.8 min		Pb-210 22.3 y	Pb-206 Stable lead isotope			Pb-212 10.6 hrs	36%	Pb-208 Stable lead isotope			Pb-211 36.1 min	Pb-207 Stable lead isotope
Thallium											Tl-208 3.05 min				Tl-207 4.77 min

Secular Equilibrium




At steady state; $\lambda_P[P] = \lambda_D[D]$ or $A_p = A_d$

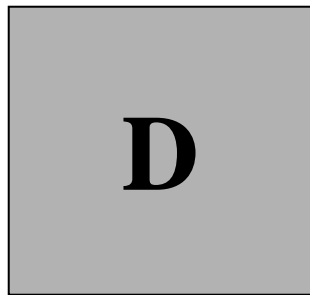
Scavenging



[e.g soluble long-lived ^{238}U with constant A in the Ocean]



$\lambda_P[P] = A_p$



Scavenging (F)
[e.g adsorption of Th onto sinking particles]



$\lambda_D[D] = A_d$

At steady state; $A_p = A_d + F$

Scavenging and Decay

- Both first order processes
- If decay dominant then $A_P = A_D$
- Where both are important $A_D < A_P$
- Under steady state conditions the activity ratio can be used to estimate the scavenging rate and hence scavenging residence time

Equations for Scavenging Rate

$$\lambda_P[P] = \lambda_D[D] + F_D[D]$$

$$A_D/A_P = \lambda_D[D]/\lambda_P[P] = \lambda_D/(\lambda_D + F)$$

Where λ_P = decay constant for parent

λ_D = decay constant for daughter

[] = atom concentration

F = scavenging rate constant

Equations for Scavenging Rate (cont.)

Solving for F:

$$F = [(1 - A_D/A_P)/(A_D/A_P)] \lambda_D$$

or

$$\tau_{1/2} = [(A_D/A_P)/(1 - A_D/A_P)] t_{D1/2}$$

Where $\tau_{1/2}$ = scavenging “half-life”

$t_{D1/2}$ = half-life of daughter

Table 4-4. Typical activity ratios for daughter-parent pairs in various water types.

	Estuaries	Coastal	Surface Ocean	Deep Sea
$^{210}\text{Pb}/^{226}\text{Ra}$	-	-	>1*	0.4-1.0
$^{230}\text{Th}/^{234}\text{U}$	-	-	$<3 \times 10^{-5}$	3×10^{-4}
$^{228}\text{Th}/^{228}\text{Ra}$	0.01	0.05	0.2	0.5-1.0
$^{234}\text{Th}/^{238}\text{U}$	0.2	0.6	>0.9	~ 1
$^{231}\text{Pa}/^{235}\text{U}$	-	-	-	2×10^{-3}
$^{210}\text{Po}/^{210}\text{Pb}$	-	-	0.5	1.0

*Although ^{210}Pb is being removed from surface water by particles, it has an additional source. Radon atoms escaping to the atmosphere from continental soils decay to ^{210}Pb . These ^{210}Pb atoms are incorporated into aerosols and are brought back to the earth's surface by rain and aerosol impact. The flux of these atoms to the sea surface exceeds by about a factor of 10 the in situ production by radiodecay of ^{226}Ra in the upper 200 meters of the ocean.

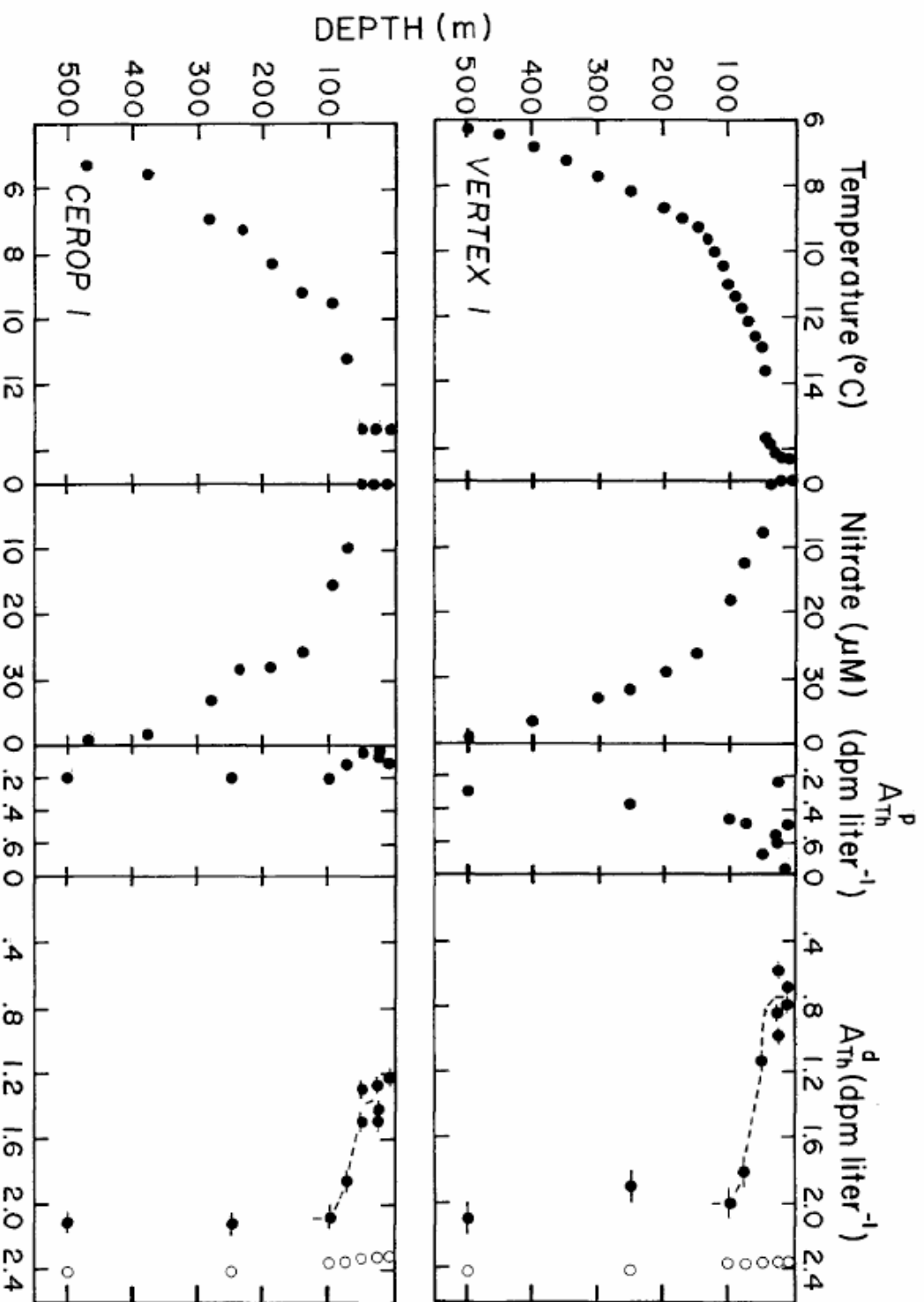


Fig. 2. Vertical profiles of temperature, nitrate, particulate and dissolved ^{234}Th activity (A_{Th}^{p} and A_{Th}^{d}) for VERTEX I and CEROP I, II, and III. ^{238}U activity—O.

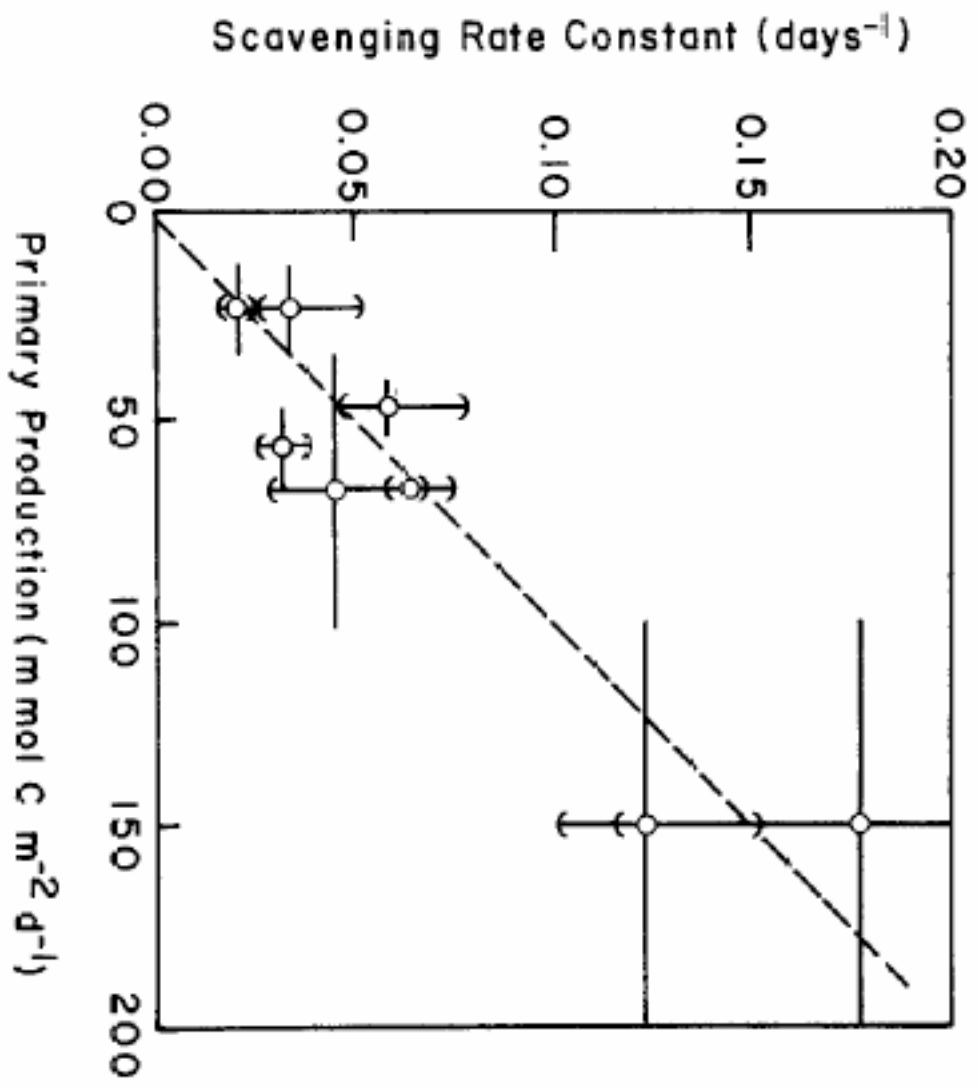
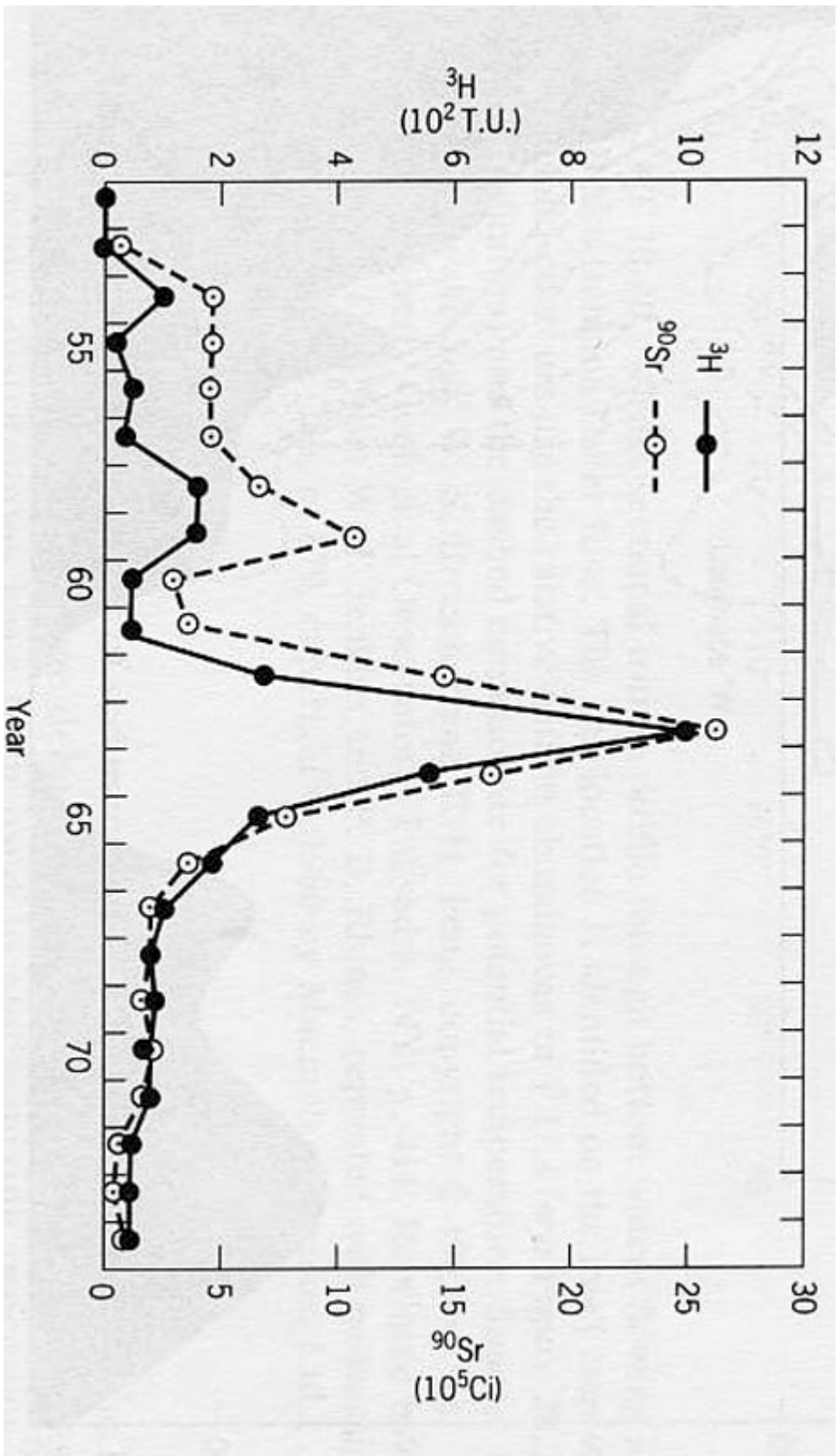
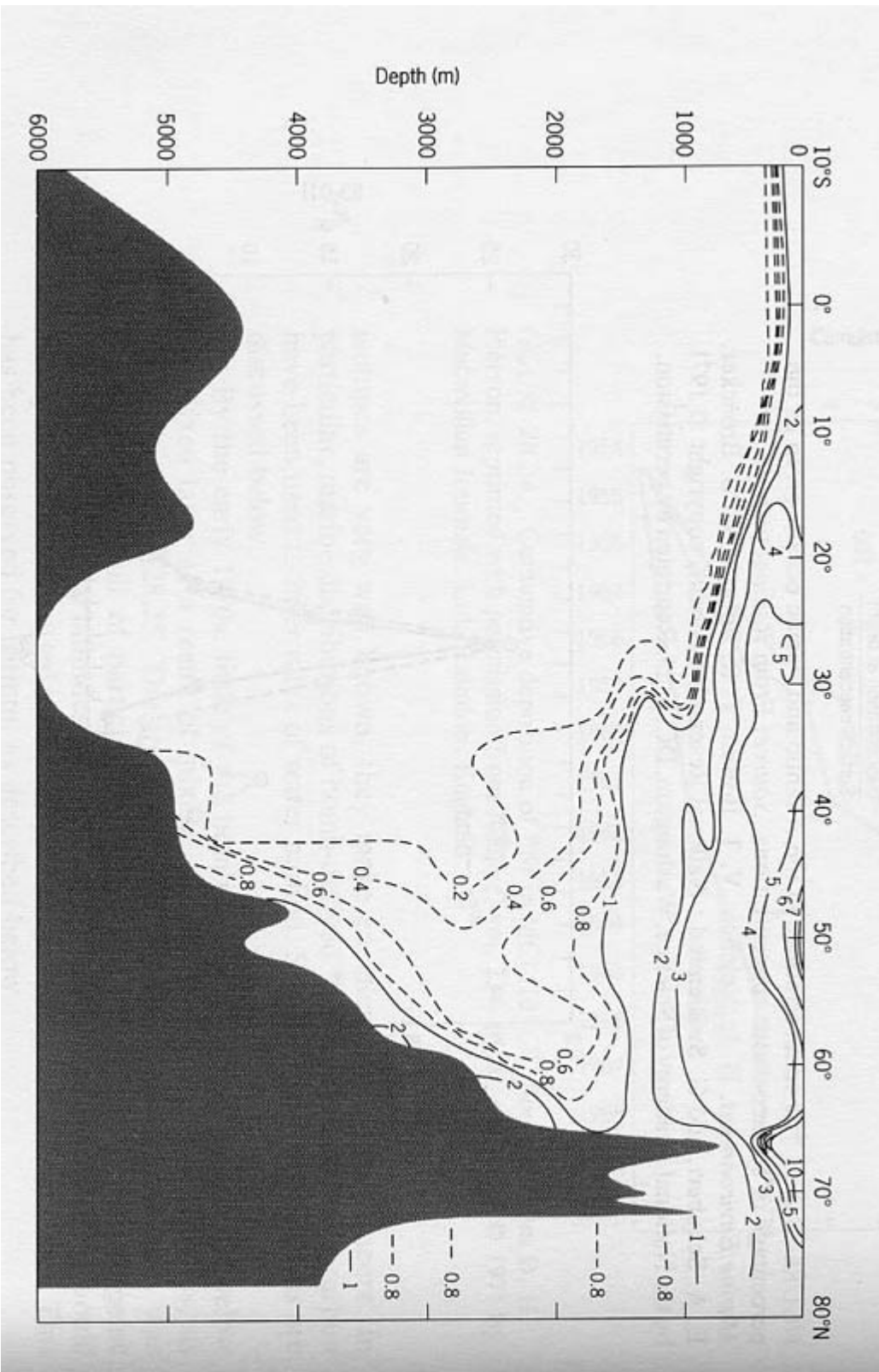


Fig. 3. Model-derived first-order dissolved ²³⁴Th scavenging rate constant vs. primary production.





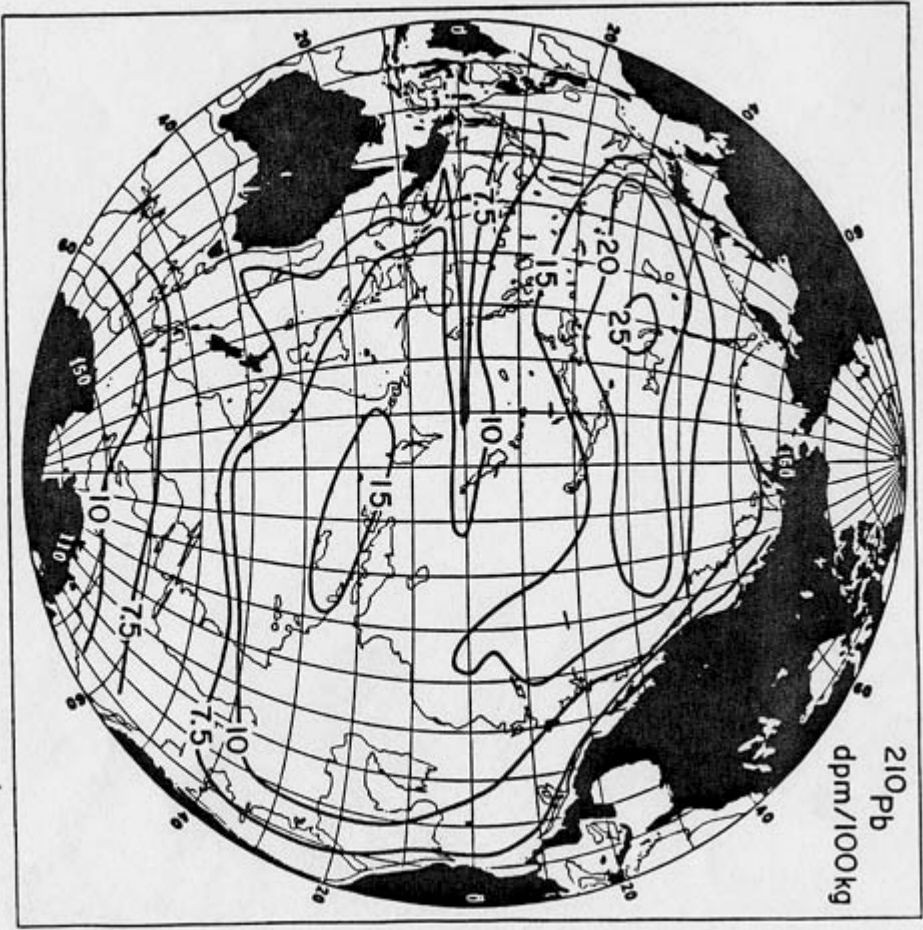


Figure 4-16. Map showing the distribution of ^{210}Pb concentrations (4m dpm/100 kg) in the surface waters of the Pacific Ocean. The results were summarized by Nozaki, Thompson and Turekian (1971).